

Probing Lorentz Invariance Violation with Neutrino Factories

F. Rossi-Torres^{a,1}

¹Instituto de Física Gleb Wataghin, Universidade Estadual de Campinas - UNICAMP, Rua Sérgio Buarque de Holanda, 777, 13083-859, Campinas-SP, Brazil

06/01/2014

Abstract In this article we show the modification in the number of neutrino events ($\nu_\mu + \bar{\nu}_\mu$) caused by Lorentz Invariant Violation (LIV), $\sigma = 5 \times 10^{-24}$ and 10^{-23} , in neutrino oscillation for a neutrino factory at a distance of 7500 km. The momentum of the muons can vary from 10-50 GeV and we consider 2×10^{20} decays per year. The modifications in the number of events caused by this σ LIV parameter could be a strong signal of new physics in a future neutrino factory.

1 Introduction

A certain type of neutrino beam is generated by a muon source of very high intensity. These muons would be stored and would decay in a ring containing a long straight section that points in the desired direction. This kind of system was historically called as *neutrino factory* and its main foundations were first developed by S. Geer [1]. The possible development of neutrino factories promises to increase the precision of neutrino oscillation parameters, assist in the determination of CP violation and also determine the hierarchy of neutrinos.

In Geer's seminal article it was pointed out several improvements in neutrino beams experiments that could be done using neutrino factories. Improvements in the determination of the ν_e and ν_μ fluxes, since these are important sources of systematic errors. Also a more "pure" beam could be obtained, since the ν_μ is contaminated by ν_e from K^+ three body decay in other experiments based on neutrino beams. All this "contamination" makes very difficult the precision experimentation in neutrino oscillation physics.

Several proposals of neutrino factories were made [2], but its realization is still far from happening, despite the fact of great effort and advances in research and developing. Recent

reviews on neutrino factories and their possible capabilities and physical potentials can be found in [3, 4].

The principle of Lorentz invariance tell us that equations, which describe some nature physical phenomena, have the same structure in all reference frames. So, if we find some system with violation of this principle, it would be an evidence of new physics and the possibility for theoretical development in the understanding of the most basic physical laws. There are several proposals and tests involving Lorentz invariance violation (LIV) [5, 6]. For a very recent review on tests of LIV in effective quantum field theories and the gravity sector, see [7]. Despite this fact, we do not have a compelling evidence of LIV and its effects are supposed to be very small and suppressed by the Planck scale ($M_p \sim 10^{19}$ GeV). Nowadays we have limits on LIV based on experiments with electrons, other charged leptons, photons and neutrons. For a complete and resumed list of these limits, see [8]. Generally these limits are put in a general framework called Standard-Model extension (SME) [9, 10] that is an extension of the Standard Model with Lorentz violating terms in the Lagrangian. Recent global model for neutrino oscillations based on the SME has shown consistency with all compelling data from accelerator, atmospheric, reactor and solar neutrino experiments and even reproduces the anomalous low-energy excess observed in MiniBooNE [11, 12].

Neutrinos can play an important role in this LIV picture [13–15]. One of the ways of determining the LIV is measuring the neutrino (ν) time of flight [15]. For example, such kind of measurement was done by the MINOS experiment [16], where they have compared the detection times in the near and far detectors of 3 GeV neutrino beams. The result was $(\nu - c)/c = 5.1 \pm 2.9 \times 10^{-5}$ at 68% C.L. Also the OPERA experiment determined in a recent analysis that $-1.8 \times 10^{-6} < (\nu - c)/c < 2.3 \times 10^{-6}$ at 90% C.L [17]. Other two experiments recently determined the neutrino ve-

^ae-mail: ftorres@ifi.unicamp.br

locity: ICARUS with $\delta t = \delta t_c - \delta t_v = 0.10 \pm 0.67 \pm 2.39$ ns [18] and LVD with $-3.8 \times 10^{-6} < (v - c)/c < 3.1 \times 10^{-6}$ at 99% C.L [19].

Another way to investigate LIV is making use of neutrino oscillation, since there will be modifications in the energy-momentum relation of the particle and therefore its Hamiltonian will be modified [20]. Models of string theory and extra dimensions have also explored the LIV possibility by the breaking of CPT symmetry. If CPT is violated, then there will be differences in the oscillation probabilities of neutrinos compared with the ones of antineutrinos. This possibility was investigated in the context of neutrino factories in [21, 22].

In this work we investigate the modification in the total detected number of events ($\nu_\mu + \bar{\nu}_\mu$) by the introduction of the LIV parameter in neutrino oscillation for a neutrino factory with 2×10^{20} muon decays per year localized in a distance of 7500 km of the detector. The muons are accelerated until they reach a momentum which varies from 10 GeV/c to 50 GeV/c and, according to our calculations, modifications in the number of events happen for $\sigma \neq 0$, since there is modification in the oscillation pattern. For the oscillation to be modified by the Lorentz violating parameter, which we call here σ_i , we must have $E\delta\sigma_{ij}L \approx \pi$. So taking a distance L of 1000 km, for example, and an energy E of about 10 GeV, $\delta\sigma_{ij}$ must be about 10^{-23} .

This article is organized as follows: in Sec. 2 we present the main principles of the production of neutrinos in a neutrino factory; in Sec. 3 and sec. 4, we describe the neutrino propagation and its interaction with the matter of the Earth including the LIV parameter, culminating with its detection. In Sec. 5, we present our results, showing the number of events for the situations with the inclusion of the LIV parameter σ and the standard situation with no Lorentz violation ($\sigma = 0$). Finally, we conclude our work in Sec. 6.

2 Neutrino production

As pointed out in [23], neutrino factories have basic concepts enumerated as followed: (i) a pion source which is produced by a multi-GeV proton beam (produced by a multi-MW proton source) focused in a particular target; (ii) secondary charged pions radially confined by a high-field target solenoid; (iii) production of positive and negative muons by decay of pions in a long solenoidal channel; (iv) capture of muons by rf cavities and reductions of the spreading in energy; and (v) a reduction of the transverse momentum of the muons in an ionization cooling channel. We are not going to detail the neutrino factory R&D. For more information about this, see [3, 4].

In a general neutrino factory, neutrinos are produced by μ^\pm decay. All flavors are produced in a neutrino factory,

except ν_τ and $\bar{\nu}_\tau$. We have the following decays: $\mu^- \rightarrow e^- + \bar{\nu}_e + \nu_\mu$ and $\mu^+ \rightarrow e^+ + \nu_e + \bar{\nu}_\mu$. In the muon rest frame, we can write the distribution of $\bar{\nu}_\mu$ (ν_μ) in the following expression [24, 25]:

$$\frac{d^2 N_{\bar{\nu}_\mu}}{dy d\Omega} = \frac{2y^2}{4\pi} [(3 - 2y) \mp (1 - 2y) \cos \theta], \quad (1)$$

where $y \equiv 2E/m_\mu$, E represents the neutrino energy and m_μ is the muon rest mass; θ is the angle between the neutrino momentum vector and the muon spin direction. In Eq. (2), we show the expression for the distribution of ν_e ($\bar{\nu}_e$):

$$\frac{d^2 N_{\nu_e}}{dy d\Omega} = \frac{12y^2}{4\pi} [(1 - y) \mp (1 - 2y) \cos \theta]. \quad (2)$$

For simplicity we are going to consider here unpolarized muon beams, so Eqs. (1) and (2) become $\frac{d^2 N_{\bar{\nu}_\mu}}{dy d\Omega} = \frac{2y^2}{4\pi} (3 - 2y)$ and $\frac{d^2 N_{\nu_e}}{dy d\Omega} = \frac{12y^2}{4\pi} (1 - y)$. We will consider 2×10^{20} μ^\pm decays per year. The μ^\pm momentum in our neutrino factory will vary from 10 GeV/c to 50 GeV/c. It is important to notice that recently in Ref. [26] there was a proposition of a very low energy neutrino factory, where the muon energy is about 2-4 GeV and in [27], Sec. III-IV, there is a discussion about the setup/optimization and the systematics of this low energy neutrino factory.

3 Neutrino Propagation

After the production, neutrinos will propagate through Earth and will travel a distance (L) of about 7500 km, approximately the distance from Fermilab to Gran Sasso. We know that those neutrinos will oscillate during their propagation and will suffer MSW effects [28]. This L baseline is usually known as the “magic” baseline [29], because is the distance that, in principle, can help to solve the unknown neutrino mass ordering and improve, for example, the determination of θ_{13} ¹. For studies of Earth matter effects in very long baselines neutrino oscillations, such as neutrino factories, see [30, 31]. The equation of evolution, in flavor basis and using natural units ($c = 1$ and $\hbar = 1$), is written by

$$i \frac{d\Psi_\alpha}{dx} = H_f \Psi_\alpha, \quad (3)$$

where $\Psi_\alpha = (\Psi_{\alpha e} \ \Psi_{\alpha \mu} \ \Psi_{\alpha \tau})$, for $\alpha = e, \mu, \tau$, and x is the neutrino position. The effective Hamiltonian ($H_{eff} \equiv H_f$) in this case includes the Earth matter effects, represented by the function $A(x)$, which contains the charged current interactions of neutrinos with the electrons on Earth:

$$A(x) = 2\sqrt{2}EG_F n_e(x), \quad (4)$$

¹In [29], if there is a combination of this 7500 km baseline with another baseline of 3000 km, it is also going to be used to determine CP violation phase.

where E represents the neutrino energy, G_F is the Fermi coupling constant ($G_F = 1.166 \times 10^{-5} \text{ GeV}^{-2}$) and $n_e(x)$ represents the electronic density, which depends on the neutrino position along its path. Considering $n_e(x)$ a spherically symmetric distribution, the core and the mantle are the two main parts; besides those two, there are shells and other layers. The Earth radius is about 6371 km and the core has a radius of 3486 km. The mantle has 2885 km of depth. The neutrino path in Earth is determined by the nadir angle (θ_n). For $\theta_n \leq 33.17^\circ$, or $L \geq 10660$ km, neutrinos will cross the core. Since we are considering distances less than this particular value, our neutrino path crosses only the mantle region, which has an average density of $\bar{n}_e^{\text{mantle}} \approx 2.2N_A \text{ cm}^{-3}$ [32], where N_A is the Avogadro number. As it was developed in [33–35], since there is no significant change in the electronic density, we consider $n_e(x)$ constant along the neutrino path and equals to the average: $n_e(x) = \bar{n}_e^{\text{mantle}}$. So, for now on we are going to represent $A(x) \equiv \bar{A}$. For modifications in the oscillations using a non-constant profile see [36], where there are some changes in the oscillation probabilities, however they are only of a few percent.

Back to H_{eff} , we can write it as $H_{eff} \equiv H_f = UHU^\dagger + \bar{A}$, where U is the PMNS mixing matrix, characterized by four parameters: θ_{12} , θ_{23} , θ_{13} and δ , the phase related with possible CP-violation, H is the Hamiltonian in the mass eigenstates basis, $(\nu_1 \nu_2 \nu_3)$, and it is related with the LIV modification, since for a general mass eigenstate i we can write:

$$E_i \approx (1 + \sigma_i)E + \frac{m_i^2}{2E}, \quad (5)$$

where we considered $m_i \ll p_i$, m_i is the mass of each mass eigenstate and p_i is their respective momentum, for $i = 1, 2, 3$. The LIV parameter is represented by σ_i in first order approximation. For $\sigma_i = 0$, we recover the usual and standard dispersion relation for a neutrino in the ultra-relativistic approximation. This σ will represent a small perturbation in the dispersion relation when we break the Lorentz invariance of some Lagrangian. In this article we do not show any Lagrangian with Lorentz breaking term, but we invite the reader to look for more theoretical motivation of this kind of phenomena in [20], for example. So the Hamiltonian in the mass basis is going to be explicitly written as:

$$H = E + \begin{pmatrix} 0 & 0 & 0 \\ 0 & E(\sigma_2 - \sigma_1) + \frac{\Delta m_{21}^2}{2E} & 0 \\ 0 & 0 & E(\sigma_3 - \sigma_1) + \frac{\Delta m_{31}^2}{2E} \end{pmatrix}. \quad (6)$$

For the distance considered and the energy range of order of tens of GeV, we can ignore the CP violation effects [27, 37]. In Eq. (6), we are going to consider, for simplicity, that the LIV modifications are $\sigma_i - \sigma_j \equiv \sigma$. Also $\Delta m_{ij}^2 \equiv m_j^2 - m_i^2$, for $j = 1, 2, 3$. We are going to consider the best-fit parameters of the oscillation parameters determined by [38]. By the solar experiments and KamLand reactor $\bar{\nu}_e$, $\Delta m_{21}^2 = 7.54 \times$

10^{-5} eV^2 and $\sin^2 \theta_{12} = 0.307$ are the best-fit values. For normal hierarchy (NH), $\Delta m_{32}^2 = 2.43 \times 10^{-3} \text{ eV}^2$, $\sin^2 \theta_{23} = 0.386$ and $\sin^2 \theta_{13} = 0.0241$. For inverted hierarchy (IH), we use the following oscillation parameters: $\Delta m_{32}^2 = 2.42 \times 10^{-3} \text{ eV}^2$, $\sin^2 \theta_{23} = 0.392$ and $\sin^2 \theta_{13} = 0.0244$. These parameters are fully summarized in Table 1.

	$\Delta m_{21}^2 \text{ (eV}^2\text{)}$	$\Delta m_{31}^2 \text{ (eV}^2\text{)}$	$\sin^2 \theta_{21}$	$\sin^2 \theta_{23}$	$\sin^2 \theta_{13}$
NH	7.54×10^{-5}	2.43×10^{-3}	0.307	0.386	0.0241
IH	7.54×10^{-5}	2.42×10^{-3}	0.307	0.392	0.0244

Table 1 Values of the best-fit oscillation parameters extracted from the Bari group [38].

We are going to calculate the conversion probabilities for the so-called *golden channel*, $\nu_e \rightarrow \nu_\mu$ and $\bar{\nu}_e \rightarrow \bar{\nu}_\mu$. Also, we are going to calculate the survival probabilities for the $\nu_\mu \rightarrow \nu_\mu$ and $\bar{\nu}_\mu \rightarrow \bar{\nu}_\mu$ channels. These are justified since we are interested in events related to the productions of μ^\pm in the detector and only ν_μ and $\bar{\nu}_\mu$ are going to generate these muons, as we are going to detail in next section. The extraction of the probabilities for each neutrino energy, which varies from 1 GeV to 50 GeV, and for the fixed baseline of $L = 7500$ km, is done by solving numerically the differential equation shown in Eq. (3). The initial condition for $\nu_e \rightarrow \nu_\mu$ (or $\bar{\nu}_e \rightarrow \bar{\nu}_\mu$) are $\Psi_e(0) = (\Psi_{ee} \ \Psi_{e\mu} \ \Psi_{e\tau}) = (1 \ 0 \ 0)$. In the other hand, for $\nu_\mu \rightarrow \nu_\mu$ (or $\bar{\nu}_\mu \rightarrow \bar{\nu}_\mu$) are $\Psi_\mu(0) = (\Psi_{\mu e} \ \Psi_{\mu\mu} \ \Psi_{\mu\tau}) = (0 \ 1 \ 0)$.

We will also consider the different effects of the ordering of the neutrino masses. We must remember that this question is still an open one in neutrino physics. *Normal hierarchy* (NH) is considered when we have the lightest mass eigenstates being m_{ν_1} and the heaviest, m_{ν_3} : $m_{\nu_1} < m_{\nu_2} \ll m_{\nu_3}$. In the case of *inverted hierarchy* (IH) we have: $m_{\nu_3} \ll m_{\nu_2} < m_{\nu_1}$.

In Fig. 1, we plot the conversion probabilities for the channel $\nu_e \rightarrow \nu_\mu$. Solid curves represent the standard picture ($\sigma = 0$) without LIV; dashed and dotted curves are the LIV cases for $\sigma = 5 \times 10^{-24}$ and $\sigma = 10^{-23}$, respectively. Thinner curves are for normal hierarchy (NH) and thicker curves are for inverted hierarchy (IH). A few comments about the standard case ($\sigma = 0$) are in order now. We notice that the peak of the conversion probability for $\nu_e \rightarrow \nu_\mu$, in NH case, occurs around ~ 6.5 GeV, which is the resonance energy (E_{res}) for the Earth matter potential (V), the θ_{13} angle and the Δm_{31}^2 considered here: $E_{res} = \frac{\Delta m_{31}^2 \cos 2\theta_{13}}{2V}$. See that for IH case, there is a suppression in the oscillation, if one compares to the NH case, since interactions with matter are practically suppressed. In Fig. 2, we have the same pattern, but now for the *golden channel* $\bar{\nu}_e \rightarrow \bar{\nu}_\mu$. For approximately $E \geq 4$ GeV the presence of LIV σ factor changes signifi-

cantly the values of the probabilities, as we can see in Fig. 1 and 2.

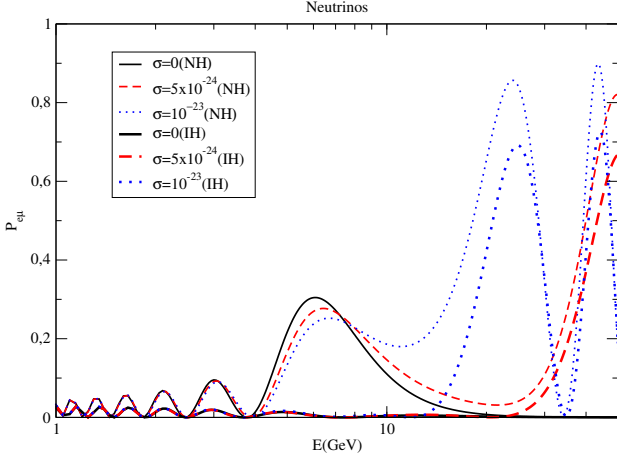


Fig. 1 In this figure we show the conversion probability for the *golden channel* $\nu_e \rightarrow \nu_\mu$. We consider a baseline of $L = 7500$ km. Solid curve is for the standard picture ($\sigma = 0$); dashed and dotted curves are the LIV cases with $\sigma = 5 \times 10^{-24}$ and $\sigma = 10^{-23}$, respectively. Thinner curves are for normal hierarchy (NH) and thicker curves are for inverted hierarchy (IH).

The presence of a new oscillation term, when we take into account σ , explains why these dotted and dashed curves have new oscillation peaks. There are modifications in the oscillation length and new resonances appear in the propagation. We stress the fact that for $\sigma \lesssim 1 \times 10^{-24}$, there is a coincidence between the LIV conversion probabilities with the standard situation ($\sigma = 0$). Of course, in the present situation and analysis, this is a very weak limit, since here no simulation of experimental data was done for the neutrino factory we are taking into account.

In Fig. 3 and Fig. 4, respectively, we show the survival probabilities for the processes $\nu_\mu \rightarrow \nu_\mu$ and $\bar{\nu}_\mu \rightarrow \bar{\nu}_\mu$. From these figures we infer that modifications between the LIV case and the standard one occur approximately for $E \geq 6$ GeV. So, we deduce that LIV can only be probed for high energy neutrino factories, since it is in this energy regime that the main modifications in the oscillation pattern occurs.

4 Neutrino Detection

Neutrinos will be detected at a far site of about $L = 7500$ km from the neutrino factory. The detection will be done using a magnetized iron detector with 10 kton, where we consider and idealize a detection efficiency of 100%. The detection is done when the ν_μ interacts with the nucleus N and produces the correlated lepton μ^- . The same happens for $\bar{\nu}_\mu$, but the lepton associated is the μ^+ . The charged-current (CC) cross sections related to these process are given by [39]

$$\sigma_{\nu N} \approx 0.67 \times 10^{-38} \times E(\text{GeV}) \text{ cm}^2 \quad (7)$$

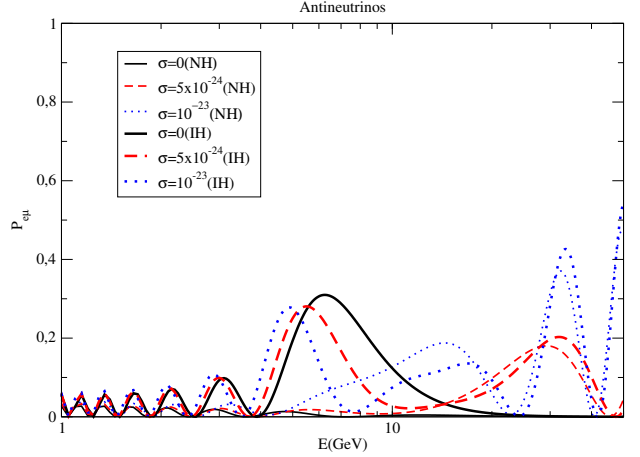


Fig. 2 In this figure we show the conversion probability for the *golden channel* $\bar{\nu}_e \rightarrow \bar{\nu}_\mu$. We consider a baseline of $L = 7500$ km. Solid curve is for the standard picture ($\sigma = 0$); dashed and dotted curves are the LIV cases with $\sigma = 5 \times 10^{-24}$ and $\sigma = 10^{-23}$, respectively. Thinner curves are for normal hierarchy (NH) and thicker curves are for inverted hierarchy (IH).

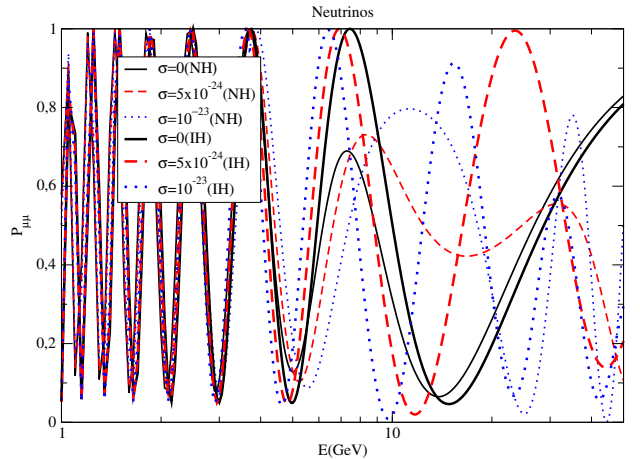


Fig. 3 In this figure we show the conversion probability for the process $\nu_\mu \rightarrow \nu_\mu$. We consider a baseline of $L = 7500$ km. Solid curve is for the standard picture ($\sigma = 0$); dashed and dotted curves are the LIV cases with $\sigma = 5 \times 10^{-24}$ and $\sigma = 10^{-23}$, respectively. Thinner curves are for normal hierarchy (NH) and thicker curves are for inverted hierarchy (IH).

and

$$\sigma_{\bar{\nu} N} \approx 0.34 \times 10^{-38} \times E(\text{GeV}) \text{ cm}^2. \quad (8)$$

One possible detector that is nowadays being considered is the one called MIND [40]. The MIND detector will be able to identify the channel of oscillation by the production of muons and their respective charge signals. We could point out an advantage of muon detection: backgrounds are very small, of order of 3×10^{-5} . This is very small if we compare with ν_e detection in superbeams experiments [41].

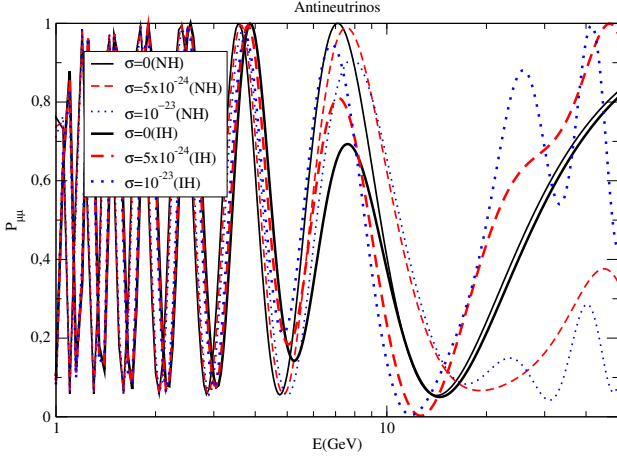


Fig. 4 In this figure we show the conversion probability for the process $\bar{\nu}_\mu \rightarrow \bar{\nu}_\mu$. We consider a baseline of $L = 7500$ km. Solid curve is for the standard picture ($\sigma = 0$); dashed and dotted curves are the LIV cases with $\sigma = 5 \times 10^{-24}$ and $\sigma = 10^{-23}$, respectively. Thinner curves are for normal hierarchy (NH) and thicker curves are for inverted hierarchy (IH).

5 Results

We consider, also in an optimistic way, a threshold for neutrino detection of 1 GeV. As pointed out before, we take into consideration in the production mechanism 2×10^{20} muon decays per year that will produce the neutrino spectra characterized by Eq. (1) and Eq. (2). After the neutrino production, we have a propagation for 7500 km along the Earth, where our σ LIV factor is going to be taken into account and we solve numerically Eq. (3). The detection of these neutrinos is represented by the cross sections in Eqs. (7,8) and we use a detector size of 10 kton.

In Fig. 5 we show the total number of events ($\nu_\mu + \bar{\nu}_\mu$) per year considering a μ^- ring for several muon momenta, which vary from 10 GeV/c to 50 GeV/c. Solid lines are for the standard case, i.e., $\sigma = 0$. Red dashed lines are for the LIV case $\sigma = 5 \times 10^{-24}$ and dotted blue lines are for the LIV case $\sigma = 10^{-23}$. The thicker lines represent the inverted hierarchy (IH) and the thinner ones the normal hierarchy (NH). The same is done in Fig. 6, but considering a μ^+ ring.

We notice from both figures that we can distinguish the rate if we consider the LIV factor from the standard case. This happens for every momentum of the muon in the neutrino factory. The main reason of these modifications is the distinct behaviour of the oscillations in LIV cases, as we can notice in Figs. 1,2,3 and 4, especially for $E > 10$ GeV, where the modifications become more pronounced.

For a better comprehension of the inclusion of the LIV parameter, we calculate the number of events for two specific momenta of the muon: $p = 20$ GeV/c and $p = 50$ GeV/c. The calculation has been made for NH and IH cases and considering different muon charges (μ^\pm). They are resumed in Table 2 and Table 3. In Table 2, for both muon polarizations

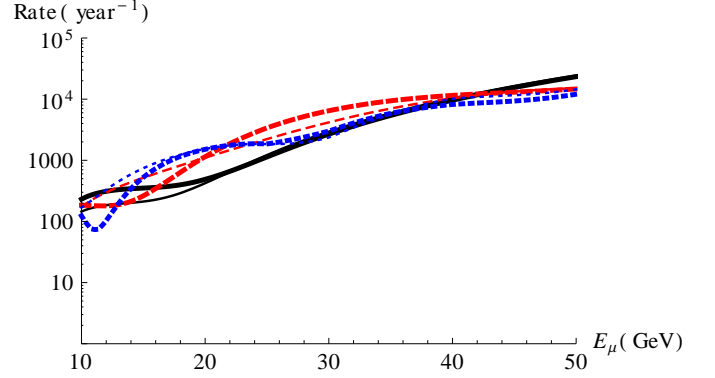


Fig. 5 Number of events, $\nu_\mu + \bar{\nu}_\mu$, per year for a 10 kton detector considering neutrinos produced in a neutrino factory with a μ^- ring for several muon momenta. The legend of our curves respects the same pattern of the other figures. That is why it has been omitted.

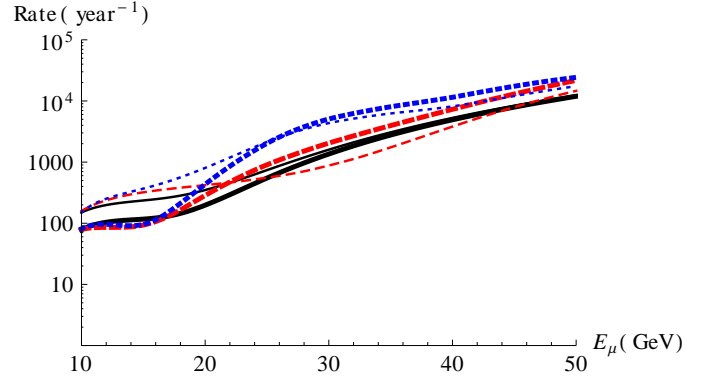


Fig. 6 The same as in Fig. 5, but for a μ^+ ring.

and both hierarchies, we notice an increase of the total number of events ($\nu_\mu + \bar{\nu}_\mu$) per year when we introduce the LIV factor. First, this increase, for μ^- ring, can be explained by the fact that in both LIV cases, $P_{e\mu}$ and $P_{\mu\mu}$ for $\bar{\nu}_e \rightarrow \bar{\nu}_\mu$ and $\nu_\mu \rightarrow \nu_\mu$, respectively, are greater than $P_{e\mu}$ and $P_{\mu\mu}$ in the non-LIV case: see Fig. 1 and Fig. 4 for regions where $E < 20$ GeV. Also, we point out that the number of events in μ^- ring is larger than in μ^+ ring. That happens because, for μ^+ ring, modifications in the probabilities curves are less drastic than in the case of the μ^- ring for $E < 20$ GeV.

In Table 3, where we evaluate the number of events ($\nu_\mu + \bar{\nu}_\mu$) per year for muons with momentum equals to 50 GeV/c, for the μ^- ring, there is a reduction in the number of events when the σ LIV parameter is $\neq 0$, since $P_{\mu\mu}$, for the oscillation channel $\nu_\mu \rightarrow \nu_\mu$, is suppressed for neutrino energies higher than 20 GeV. This suppression is even more pronounced when $\sigma = 10^{-23}$. However, in the case of a μ^+ ring, generally we can notice an increase in $P_{e\mu}$ for the process $\nu_e \rightarrow \nu_\mu$, and $P_{\mu\mu}$, for the channel $\bar{\nu}_\mu \rightarrow \bar{\nu}_\mu$. These explains the increase in the number of events compared to the non LIV case. The fact that NH has fewer events than IH, for $\sigma = 5 \times 10^{-24}$ and $\sigma = 10^{-23}$, is due to the fact that $P_{\mu\mu}$

(dotted and dashed curves), for $E > 15$ GeV, is smaller than $P_{\mu\mu}$ in the $\sigma = 0$ case (solid curve) - see Fig. 4.

Ring	Hierarchy	$\sigma = 0$	$\sigma = 5 \times 10^{-24}$	$\sigma = 10^{-23}$
μ^-	NH	422	1103	1533
μ^-	IH	488	1147	1511
μ^+	NH	349	420	803
μ^+	IH	197	285	434

Table 2 Number of events, $\nu_\mu + \bar{\nu}_\mu$, per year for 10 kton detector considering a 7500 km neutrino factory baseline for $\sigma = 0$, $\sigma = 5 \times 10^{-24}$ and $\sigma = 10^{-23}$. We consider here normal hierarchy (NH) and inverted hierarchy (IH). Calculations were also done for a μ^- ring and μ^+ ring with momentum $p = 20$ GeV/c.

Ring	Hierarchy	$\sigma = 0$	$\sigma = 5 \times 10^{-24}$	$\sigma = 10^{-23}$
μ^-	NH	24414	15057	14492
μ^-	IH	23314	14681	12043
μ^+	NH	12414	14637	17480
μ^+	IH	11908	21699	24310

Table 3 Number of events, $\nu_\mu + \bar{\nu}_\mu$, per year for 10 kton detector considering a 7500 km neutrino factory baseline for $\sigma = 0$, $\sigma = 5 \times 10^{-24}$ and $\sigma = 10^{-23}$. We consider here normal hierarchy (NH) and inverted hierarchy (IH). Calculations were also done for a μ^- ring and μ^+ ring with momentum $p = 50$ GeV/c.

6 Conclusions

In this work we analysed the possible modifications in the number of events ($\nu_\mu + \bar{\nu}_\mu$) per year in a neutrino factory localized 7500 km of a 10 kton detector when we introduce a parameter σ that breaks the Lorentz Invariant assumption. These can have consequences in neutrino oscillation mechanisms and modify the number of events. In Fig. 5 and Fig. 6 we have showed that modification in the number of events happens when one compares the standard case ($\sigma = 0$) to the LIV cases $\sigma = 5 \times 10^{-24}$ and $\sigma = 10^{-23}$ for several muon momenta, both muon polarizations and NH/IH. These parameter values were chosen considering the baseline and typical neutrino energies of a neutrino factory, since they generate clear modifications in the survival probabilities ($\nu_\mu \rightarrow \nu_\mu$ and $\bar{\nu}_\mu \rightarrow \bar{\nu}_\mu$) and in the conversion probabilities ($\nu_e \rightarrow \nu_\mu$ and $\bar{\nu}_e \rightarrow \bar{\nu}_\mu$).

In Ref. [42], considering the $\nu_\mu \leftrightarrow \nu_\tau$ oscillation channel and the Super-Kamiokande data of atmospheric neutrinos with range of energy of about four decades, the standard scenario was confirmed as the dominant effect in neutrino oscillation and other terms that induce violations in relativity as subleading effects. With the inclusion of K2K data,

Ref. [43] obtained the same conclusion. Using the Macro data of upward-going muons of atmospheric neutrinos, [44] also found that LIV is not favored by the atmospheric data, even as a subleading term in the oscillation mechanism. At 90% C.L these works found, roughly speaking, that $\sigma \lesssim 6 \times 10^{-24}$. Despite the fact atmospheric neutrinos disfavour LIV in the neutrino oscillation context, results in neutrino factories show that, if we have possible violation in the principle of Lorentz invariance, this can be detected in a future neutrino factory, since there is a good sensibility in the number of events detected. We put this in evidence considering values of σ near the upper limits experimentally determined by the results of atmospheric neutrinos, whose flux is well understood: the normalizations are known to 20% approximately (10% approximately for neutrino energies below 10 GeV) and ratio of fluxes are known to $\sim 5\%$. The atmospheric fluxes decay rapidly with neutrino energies for $E_\nu > 1$ GeV. Considering those properties known about atmospheric neutrinos and the perspective of very clean signals in neutrinos factories, we think neutrino factories in the future can achieve lower uncertainties and reveal the LIV phenomenon or put more stringent bounds on it.

Acknowledgements

The author would like to thank Conselho Nacional de Desenvolvimento Científico e Tecnológico (CNPq) for the financial support. Also, he would like to thank prof. M. M. Guzzo for reading this material and making very useful suggestions.

References

1. S. Geer, Phys. Rev. D **57**, 6989 (1998) [Erratum-ibid. D **59**, 039903 (1999)] [hep-ph/9712290].
2. Y. Kuno, Y. Mori, S. Machida, T. Yokoi, Y. Iwashita, J. Sato and O. Yasuda, “A feasibility study of a neutrino factory in Japan,” NUFACJ-05-24-2001, <http://www-prism.kek.jp/nufactj/index.html>; B. Autin, A. Blondel and J. R. Ellis, “Prospective Study of Muon Storage Rings at CERN,” CERN-99-02; The Muon Collider and Neutrino Factory Collaboration: see <http://www.cap.bnl.gov/mumu>; D. Finley and N. Holtkamp, “A feasibility study of a neutrino source based on a muon storage ring,” Nucl. Instrum. Meth. A **472**, 388 (2000). S. Ozaki, R. B. Palmer, M. S. Zisman, J. C. Gallardo, M. Goodman, A. Hassanein, J. H. Norem and C. B. Reed *et al.*, “Feasibility study 2 of a muon based neutrino source,” BNL-52623; P. Gruber, M. Aleksa, J. F. Amand, B. Autin, J. L. Baldy, M. Benedikt, R. Bennett and A. Bernadon *et al.*, “The

- study of a European Neutrino Factory complex,” CERN-PS-2002-080-PP; M. M. Alsharoa *et al.* [Muon Collider/Neutrino Factory Collaboration], “Recent progress in neutrino factory and muon collider research within the Muon collaboration,” *Phys. Rev. ST Accel. Beams* **6**, 081001 (2003) [hep-ex/0207031].
3. A. Stahl, C. Wiebusch, A. M. Guler, M. Kamiscioglu, R. Sever, A. U. Yilmazer, C. Gunes and D. Yilmaz *et al.*, CERN-SPSC-2012-021.
 4. A. Bandyopadhyay *et al.* [ISS Physics Working Group Collaboration], *Rept. Prog. Phys.* **72**, 106201 (2009) [arXiv:0710.4947 [hep-ph]].
 5. B. -Q. Ma, arXiv:1203.5852 [hep-ph].
 6. B. -Q. Ma, *Int. J. Mod. Phys. Conf. Ser.* **10**, 195 (2012) [arXiv:1203.0086 [hep-ph]].
 7. S. Liberati, *Class. Quant. Grav.* **30**, 133001 (2013) [arXiv:1304.5795 [gr-qc]].
 8. V. A. Kostelecky and N. Russell, *Rev. Mod. Phys.* **83**, 11 (2011) [arXiv:0801.0287 [hep-ph]].
 9. D. Colladay and V. A. Kostelecky, *Phys. Rev. D* **55**, 6760 (1997) [hep-ph/9703464].
 10. D. Colladay and V. A. Kostelecky, *Phys. Rev. D* **58**, 116002 (1998) [hep-ph/9809521].
 11. J. S. Diaz and V. A. Kostelecky, *Phys. Lett. B* **700**, 25 (2011) [arXiv:1012.5985 [hep-ph]].
 12. J. S. Diaz and A. Kostelecky, *Phys. Rev. D* **85**, 016013 (2012) [arXiv:1108.1799 [hep-ph]].
 13. V. A. Kostelecky and M. Mewes, *Phys. Rev. D* **69**, 016005 (2004) [hep-ph/0309025].
 14. J. S. Diaz, arXiv:1109.4620 [hep-ph].
 15. A. Kostelecky and M. Mewes, *Phys. Rev. D* **85**, 096005 (2012) [arXiv:1112.6395 [hep-ph]].
 16. P. Adamson *et al.* [MINOS Collaboration], *Phys. Rev. D* **76**, 072005 (2007) [arXiv:0706.0437 [hep-ex]].
 17. T. Adam *et al.* [OPERA Collaboration], *JHEP* **1301**, 153 (2013) [arXiv:1212.1276 [hep-ex]].
 18. M. Antonello, B. Baibussinov, P. Benetti, F. Boffelli, E. Calligarich, N. Canci, S. Centro and A. Cesana *et al.*, *JHEP* **1211**, 049 (2012) [arXiv:1208.2629 [hep-ex]].
 19. N. Y. Agafonova *et al.* [LVD Collaboration], *Phys. Rev. Lett.* **109**, 070801 (2012) [arXiv:1208.1392 [hep-ex]].
 20. S. R. Coleman and S. L. Glashow, *Phys. Rev. D* **59**, 116008 (1999) [hep-ph/9812418].
 21. S. M. Bilenky, M. Freund, M. Lindner, T. Ohlsson and W. Winter, *Phys. Rev. D* **65**, 073024 (2002) [hep-ph/0112226].
 22. J. S. Diaz, V. A. Kostelecky and M. Mewes, *Phys. Rev. D* **80**, 076007 (2009) [arXiv:0908.1401 [hep-ph]].
 23. S. Geer, arXiv:1202.2140 [physics.acc-ph].
 24. T. K. Gaisser, “Cosmic rays and particle physics,” Cambridge, UK: Univ. Pr. (1990).
 25. V. Barger, D. Marfatia and K. Whisnant, “The physics of neutrinos,” Princeton University Press (2012).
 26. C. D. Tunnell, J. H. Cobb and A. D. Bross, arXiv:1111.6550 [hep-ph].
 27. W. Winter, *Phys. Rev. D* **85**, 113005 (2012) [arXiv:1204.2671 [hep-ph]].
 28. L. Wolfenstein, *Phys. Rev. D* **17**, 2369 (1978); S. P. Mikheev and A. Y. Smirnov, *Sov. J. Nucl. Phys.* **42**, 913 (1985) [*Yad. Fiz.* **42**, 1441 (1985)].
 29. P. Huber and W. Winter, *Phys. Rev. D* **68**, 037301 (2003) [hep-ph/0301257].
 30. M. Freund, M. Lindner, S. T. Petcov and A. Romanino, *Nucl. Phys. B* **578**, 27 (2000) [hep-ph/9912457].
 31. M. Freund, P. Huber and M. Lindner, *Nucl. Phys. B* **585**, 105 (2000) [hep-ph/0004085].
 32. A. M. Dziewonski and D. L. Anderson, *Phys. Earth Planet. Interiors* **25**, 297 (1981).
 33. P. I. Krastev and S. T. Petcov, *Phys. Lett. B* **205**, 84 (1988).
 34. M. Chizhov, M. Maris and S. T. Petcov, hep-ph/9810501.
 35. S. T. Petcov, *Phys. Lett. B* **434**, 321 (1998) [hep-ph/9805262].
 36. I. Mocioiu and R. Shrock, *Phys. Rev. D* **62**, 053017 (2000) [hep-ph/0002149].
 37. V. Barger, D. Marfatia and K. Whisnant, *Phys. Rev. D* **65**, 073023 (2002) [hep-ph/0112119].
 38. G. L. Fogli, E. Lisi, A. Marrone, D. Montanino, A. Palazzo and A. M. Rotunno, *Phys. Rev. D* **86**, 013012 (2012) [arXiv:1205.5254 [hep-ph]].
 39. F. Boehm and P. Vogel, “Physics Of Massive Neutrinos,” CAMBRIDGE, UK: UNIV. PR. (1987).
 40. R. Bayes, A. Bross, A. Cervera, M. Ellis, A. Laing, F. J. P. Soler and R. Wands, *J. Phys. Conf. Ser.* **408**, 012075 (2013).
 41. V. D. Barger, S. Geer, R. Raja and K. Whisnant, *Phys. Rev. D* **63**, 113011 (2001) [hep-ph/0012017].
 42. G. L. Fogli, E. Lisi, A. Marrone and G. Scioscia, *Phys. Rev. D* **60**, 053006 (1999) [hep-ph/9904248].
 43. M. C. Gonzalez-Garcia and M. Maltoni, *Phys. Rev. D* **70**, 033010 (2004) [hep-ph/0404085].
 44. G. Battistoni, Y. Becherini, S. Cecchini, M. Cozzi, H. Dekhissi, L. S. Esposito, G. Giacomelli and M. Giorgini *et al.*, *Phys. Lett. B* **615**, 14 (2005) [hep-ex/0503015].